JPE 17-6-24

https://doi.org/10.6113/JPE.2017.17.6.1650
ISSN(Print): 1598-2092 / ISSN(Online): 2093-4718

Distributed Secondary Voltage Control of Islanded Microgrids with Event-Triggered Scheme

Qian Guo[*], Hui Cai[†], Ying Wang[*], and Weimin Chen[*]

[*,†]College of Mechanical and Electrical Engineering, China Jiliang University, Hangzhou, China

Abstract

In this study, the distributed secondary voltage control of islanded microgrids with multi-agent consensus algorithm is investigated. As an alternative to a time-triggered approach, an event-triggered scheme is proposed to reduce the communication load among inverter-based distributed generators (DGs). The proposed aperiodic control scheme reduced unnecessary utilization of limited network bandwidth without degrading control performance. By properly establishing a distributed triggering condition in DG local controller, each inverter is only required to send voltage information when its own event occurs. The compensation of voltage amplitude deviation can be realized, and redundant data exchange related to fixed high sampling rate can be avoided. Therefore, an efficient use of communication infrastructure can be realized, particularly when the system is operating in steady state. The effectiveness of the proposed scheme is verified by simulations on a microgrid test system.

Key words: Event-triggered scheme, Microgrid, Multi-agent system, Secondary voltage control

I. Introduction

The concept of microgrid has emerged to provide a solution in upgrading conventional power systems toward future energy distribution systems. With power electronic converters serving as interface devices, microgrids integrated various types of distributed energy resources and energy storage, which provided heat and power to local communities [1]-[3]. Thus, the expected electrical grid was inclined to be more distributed, intelligent, and flexible.

Reliable control of microgrid is necessary to ensure economically efficient operation and coordination of different distributed generation (DG) units. Hierarchical structure is suitable for the standardization of microgrid control, which consists of three levels: primary, secondary, and tertiary [4-6]. Flexible microgrids can operate in either grid-connected or islanded modes. When microgrid disconnects from a grid, the voltage and frequency stability are maintained by primary control, which is based on voltage amplitude and frequency droop method. However, the droop characteristic causes voltage amplitude and frequency deviations inside the microgrid [7], [8]. The secondary control ensures restoration of these load-dependent deviations after each load change with a slower dynamics response than the primary control [4].

Considering that secondary control involves communication links, its performance can be influenced by the features of adopted communication system, such as topology, protocol, and sampling rate [9], [10]. To overcome the drawback of a single point-of-failure of the centralized structure, the distributed counterpart has attracted much attention, which provided a more robust and reliable framework in terms of communication impairments [11]-[14]. Based on the cooperative control of multi-agent systems, the secondary control can be fully distributed through a sparse communication network [15]-[18].

The implementation of control and communication execution schemes is an important aspect in multi-agent cooperative control [19], [20]. Conventionally, a time-triggered strategy is selected, where the state information is exchanged among the agents periodically. The control period should be designed adequately small to assure the state error of agent is within the bound in worst cases and the resulting sampling rate is relatively high. A large amount of redundant sampled data led to a high transmission rate, which may cause network congestion due to bandwidth constraint. The event-triggered strategy has clear advantages considering the limited resources of communication system [19]. In event-triggered scheme, an execution is triggered when a state error exceeds a given threshold. The aperiodic information exchange among multiple

Manuscript received May 18, 2017; accepted Jul. 21, 2017
Recommended for publication by Associate Editor Kai Sun.
[†]Corresponding Author: caihui@cjlu.edu.cn
Tel: +86-571-86914550, China Jiliang University
[*]College of Mechanical and Electrical Engineering, China Jiliang University, China

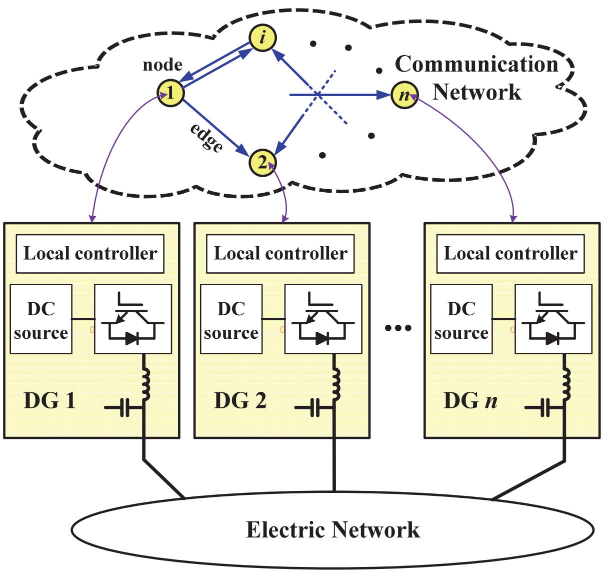

Fig.1. Islanded microgrid with distributed control structure.

agents are need-based in nature, which indicates an efficient use of communication infrastructure. Distributed cooperative control with event-triggered communication was applied to microgrids recently to facilitate power sharing among DG units [21], [22] or economic dispatch optimization [23], [24].

This study extended the event-triggered scheme to distributed secondary voltage control of islanded microgrids based on multi-agent consensus algorithm. The proposed strategy played the function of microgrid voltage restoration with reduced communication load. A Lyapunov-based technique is adopted to derive the triggering condition in DG local controller. This technique determined the event time instants in a distributed manner, which is suitable for microgrids implemented through multi-agent concept. Case studies showed that the proposed strategy can efficiently save communication resources and guarantee satisfactory performance.

The rest of this paper is organized as follows. Section II presents the distributed cooperative secondary voltage control of microgrids using multi-agent theory. Section III constructs the proposed event-triggered controller. Section IV conducts the simulations. Finally, Section V summarizes the conclusions.

II. MULTI-AGENT BASED DISTRIBUTED SECONDARY VOLTAGE CONTROL

Fig. 1 shows the general configuration of an islanded microgrid, where n DG units are connected to the electric power network of passive elements and loads. Each DG unit is composed of an energy source, an inverter, and a local controller. According to the hierarchical control scheme [4]-[6], the primary control is implemented in DG local controller, which is based on real power–frequency droop (P–f droop) and reactive power–voltage amplitude droop (Q–V droop) methods, and can provide a decentralized control capability without critical communication. Secondary control requires the interaction of DG units to correct the deviations produced by primary control, where a communication network should be facilitated to provide data exchange. In Fig. 1, the communication layout is sparse, which indicates a distributed control structure for secondary control. Each DG unit is considered as an agent, and the secondary control of the microgrid resembles the tracking synchronization problem of the multi-agent system [18].

A. Communication Network Model

The communication connections of DG units can be modeled by a digraph [15]. As shown in Fig. 1, the nodes represent the DG units and the edges denote the communication links.

In the digraph, an edge from node j to node i indicates that node i can receive the information from node j. In this condition, node j is called a neighbor of node i and communication may not be reciprocal. The set N_i denotes all the neighbors of node i. The digraph is associated with an adjacency matrix $\boldsymbol{A_G} = [a_{ij}] \in \boldsymbol{R}^{n\times n}$, where the elements formed the weight of the edges. If the edge from node j to node i exists, $a_{ij} = 1$, otherwise $a_{ij} = 0$. The in-degree matrix $\boldsymbol{D_{in}} = \mathrm{diag}\{d_i\}$ is diagonal with $d_i = \sum_{j\in N_i} a_{ij}$, and the Laplacian matrix is defined as $\boldsymbol{L_G} = \boldsymbol{D_{in}} - \boldsymbol{A_G}$. Every row sum of $\boldsymbol{L_G}$ is zero, which indicates its eigenvalue is zero, and $\boldsymbol{1_n} = [1, 1, ..., 1]^{\mathrm{T}} \in \boldsymbol{R}^{n\times 1}$ is the corresponding right eigenvector. Assuming that the digraph contains a directed spanning tree, zero is a simple eigenvalue of $\boldsymbol{L_G}$ [25], [26].

The distributed secondary voltage control based on cooperative control of multi-agents requires that the communication digraph contains a spanning tree [17], [18]. Different criteria, such as minimal link numbers and minimal link lengths, can be adopted for the selection of communication topology in practical microgrids.

B. Distributed Secondary Voltage Control

The voltage droop control equation in the primary control level is expressed as follows [27]:

$$v_i = V_0 - n_{qi} Q_i , \tag{1}$$

where V_0 is the rated value of DG voltage amplitude, Q_i is the measured reactive power after a low-pass filter (LPF), and n_{qi} is the reactive power droop coefficient. The resulting v_i is the voltage amplitude reference for the inner voltage controller of the i-th DG unit. Considering that the dynamics of droop controller is slower than that of inner voltage and current controllers, DG units can be regarded as controllable voltage sources given that output voltage amplitude v_{oi} will follow reference value v_i.

The secondary voltage control is employed to compensate the load-dependent deviation of DG output voltage amplitude due to droop characteristic. The secondary voltage control provides a compensation signal for primary control as a control reference, which shifts the *Q-V* droop response by changing the DG no-load voltage from V_0 to V_i^* in (1). With input-output feedback linearization, the secondary voltage control can be regarded as a tracking synchronization problem for a first-order multi-agent system [18]. Therefore, the secondary control operates in a distributed manner to synchronize the voltage amplitudes of all DG units to a nominal value. The regulation for V_i^* is implemented in the local controller of the *i*-th DG unit, which is expressed in the following form [18]

$$V_i^* = \int \left(n_{qi}\dot{Q}_i - c_v e_{vi} \right) dt \, , \tag{2}$$

where c_v is the secondary voltage control gain, and e_{vi} is the local neighborhood tracking error calculated as

$$e_{vi} = \sum\nolimits_{j\in N_i} a_{ij}\left(v_{oi} - v_{oj} \right) + g_i\left(v_{oi} - v_{ref} \right), \tag{3}$$

where a_{ij} is the element of adjacency matrix $\boldsymbol{A_G}$ for the communication digraph. The pinning gain $g_j = 1$ is satisfied when the *i*-th DG unit provided voltage reference v_{ref}, otherwise $g_j = 0$. The pinning gain is non-zero for at least one DG unit. In (3), each DG unit is only required to process its local and neighbor voltage information to update its own tracking error. Thus, the controller is fully distributed. With (2), the global neighborhood tracking error vector $\boldsymbol{e_v} = [e_{v1}, e_{v2}, \ldots, e_{vn}]^T$ asymptotically goes to zero. Therefore, all DG units synchronized the output voltage amplitude to reference v_{ref}, and the voltage deviation induced by *Q-V* droop control is compensated.

This coordinated control is realized by voltage state information exchange among DG units. A practical way is to implement the conventional time-triggered control with periodic sampling and transmission, where each DG unit sends the sampled voltage state to other nodes in every pre-designed control periods. The control period is generally selected with a small value to meet the requirements of worst cases, which released a large number of redundant transmission data to the communication network. By contrast, the time-triggered approach used the same control frequency for transient and steady states. Considering that the aim of secondary control is to compensate the deviations after each load change or generation inside the microgrid, executing the control task periodically during the steady operation of microgrid wastes computation and communication resources.

III. Proposed Event-Triggered Control Scheme

In event-triggered control scheme, an event occurs and the control task is executed when the pre-defined triggering condition is satisfied. The corresponding time instant is called an event time instant.

A. Proposed Event-Triggered Controller

To preserve limited communication resources and retain control performance, an event-triggered control scheme for distributed secondary voltage control of islanded microgrids is proposed. Each DG unit only transmits voltage information at its own event time instants, and the communication load is reduced. With a distributed triggering condition implemented in DG local controller, DG units generally have different event time instants, as shown in Fig. 2. The sequence of event time instants of the *i*-th DG unit in temporal order are denoted by

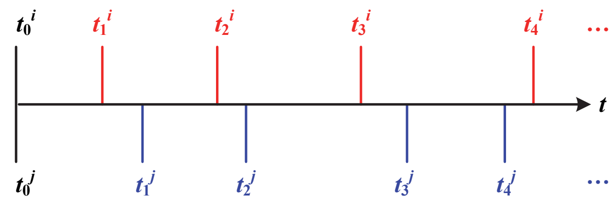

Fig. 2. Event time sequences of the *i*-th and the *j*-th DG units.

$$t_0^i < t_1^i < t_2^i < \cdots < t_k^i < \cdots . \tag{4}$$

These event time instants are instants when the event condition of the *i*-th DG unit is satisfied. The event condition will be developed in Section III-B.

The proposed distributed secondary voltage control with event-triggered scheme is expressed as

$$\begin{cases} V_i^* = \int \left(n_{qi}\dot{Q}_i(t) - c_v \hat{e}_{vi}(t) \right) dt \\ \hat{e}_{vi}(t) = \sum\nolimits_{j\in N_i} a_{ij}\left(\hat{v}_{oi}(t) - \hat{v}_{oj}(t) \right) + g_i\left(\hat{v}_{oi}(t) - v_{ref} \right) \end{cases}, \tag{5}$$

where V_i^* is the compensation signal. $\hat{e}_{vi}$ is the local neighborhood tracking error. $\hat{v}_{oi}$ is the sampled output voltage of the *i*-th DG unit at the latest event time instant $t_{k_i}^i$ to current time *t*, which can be defined as

$$\begin{cases} \hat{v}_{oi}(t) = v_{oi}\left(t_{k_i}^i \right), \quad t \in \left[t_{k_i}^i, t_{k_i+1}^i \right) \\ k_i = \arg\max_{k\in N} \left\{ t_k^i \,\middle|\, t_k^i \le t \right\} \end{cases}. \tag{6}$$

The sampled output voltage $\hat{v}_{oi}$ is maintained constant in a zero-order manner between two consecutive event time instants. Eq. (5) is based on the own voltage information of each DG and its neighbors in the communication digraph, which provided a distributed controller without central processing. Each DG unit considered its own last sampled voltage and all its neighboring DG units. Thus, for the *i*-th DG unit, the local neighborhood tracking error $\hat{e}_{vi}$ updates at its own event times and all its neighbors.

The neighborhood tracking error in the vector form is written as

$$\boldsymbol{\hat{e}_v} = \left(\boldsymbol{L_G} + \boldsymbol{G} \right)\left(\boldsymbol{\hat{v}_o} - v_{ref}\boldsymbol{1_n} \right), \tag{7}$$

where the diagonal matrix $\boldsymbol{G}$ = diag$\{g_i\} \in \boldsymbol{R}^{n\times n}$ reflects the pinning gains associated with DG units given the voltage reference.

According to the voltage droop equation, the dynamic of output voltage amplitude v_{oi} is

$$\dot{v}_{oi} = \dot{V}_i^* - n_{qi}\dot{Q}_i = -c_v \hat{e}_{vi} \, . \tag{8}$$

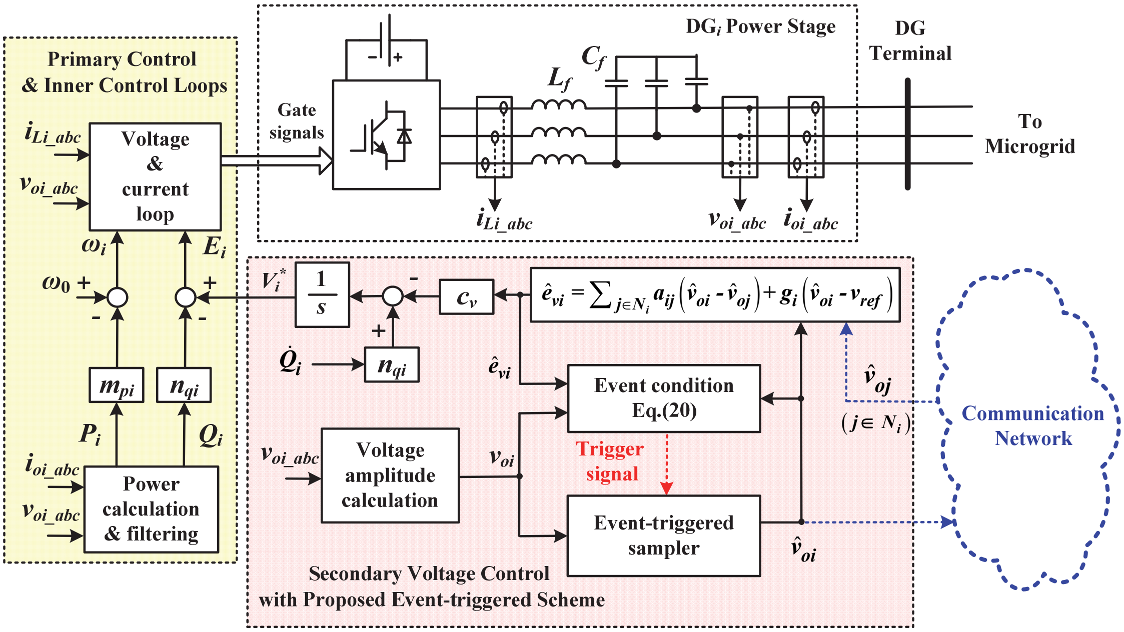

Fig. 3. Proposed event-triggered scheme for distributed secondary voltage control of islanded microgrids.

The actual output voltage amplitude v_{oi} varies with time, and correspondingly the state measurement error in voltage amplitude of the i-th DG unit with respect to the last event occurred can be defined as

$$\delta_i(t) = \hat{v}_{oi}(t) - v_{oi}(t). \tag{9}$$

The state measurement error δ_i describes the difference between the sampled and real-time output voltage. δ_i is reset to zero for every event time instant of the i-th DG unit.

By comparing (5) with (2)–(3), the proposed control strategy regulates DG voltage with sampled voltage of neighboring DG units at their event times. Hence, each DG unit only executes voltage information transmission when its event occurs rather than sending the measured voltage state periodically. The amount of resultant communication is reduced significantly without affecting the performance for secondary control of voltage restoration because the numbers of occurred events can be limited with a proper event condition.

B. Event Condition Design

The event condition design involves the selection of appropriate event time instants. The event condition aids in enforcing state measurement error δ_i to have a small magnitude. Then, the proposed secondary voltage control law of (5) is effective using $\hat{v}_{oi}$ instead of v_{oi}. Moreover, a distributed formulation for event condition is preferred, which indicated that the DG unit can determine the event time instants based on information of its own and neighboring DG information.

To derive the event condition, a Lyapunov function candidate is considered

$$V = \frac{1}{2}\left(\boldsymbol{v_o} - v_{ref}\mathbf{1_n}\right)^T \boldsymbol{P}\left(\boldsymbol{v_o} - v_{ref}\mathbf{1_n}\right), \tag{10}$$

where $\boldsymbol{P}$ = diag{$1/w_i$} is a positive definite matrix. The elements of this function satisfy $(\boldsymbol{L_G} + \boldsymbol{G})\boldsymbol{w} = \mathbf{1_n}$, where $\boldsymbol{w} = [w_1, w_2, ..., w_n]^T \in \boldsymbol{R}^{n\times 1}$ [18]. $\boldsymbol{v_o}=[v_{o1}, v_{o2}, \dots, v_{on}]^T$ is the output voltage vector.

Then, based on (7)-(8), the time derivative of Lyapunov function yields

$$\begin{aligned}\dot{V} &= \left(\boldsymbol{v_o} - v_{ref}\mathbf{1_n}\right)^T \boldsymbol{P}\dot{\boldsymbol{v}}_{\boldsymbol{o}} = \left[\boldsymbol{v_o} - v_{ref}\mathbf{1_n}\right]^T \boldsymbol{P}\left(-c_v\hat{\boldsymbol{e}}_{\boldsymbol{v}}\right) \\ &= -c_v\left[\boldsymbol{v_o} - v_{ref}\mathbf{1_n}\right]^T \boldsymbol{P}\left[-\left(\boldsymbol{L_G}+\boldsymbol{G}\right)\left(\hat{\boldsymbol{v}}_{\boldsymbol{o}} - v_{ref}\mathbf{1_n}\right)\right]\end{aligned}. \tag{11}$$

Based on the definition in (9), and denote $\boldsymbol{z} = \hat{\boldsymbol{v}}_{\boldsymbol{o}} - v_{ref}\mathbf{1_n}$, (11) can be rewritten as

$$\begin{aligned}\dot{V} &= -c_v\left(\boldsymbol{z}-\boldsymbol{\delta}\right)^T \boldsymbol{P}\left[-\left(\boldsymbol{L_G}+\boldsymbol{G}\right)\boldsymbol{z}\right] \\ &= -c_v\left[\boldsymbol{z}^T\boldsymbol{P}\left(\boldsymbol{L_G}+\boldsymbol{G}\right)\boldsymbol{z} + \boldsymbol{\delta}^T\boldsymbol{P}\left(\boldsymbol{L_G}+\boldsymbol{G}\right)\boldsymbol{z}\right]\end{aligned}. \tag{12}$$

Using the inequality $xy \le (1/2a)x^2 + (a/2)\,y^2$, for $a > 0$, (12) has an upper bound shown as

$$\dot{V} \le -c_v\boldsymbol{z}^T\boldsymbol{P}\left(\boldsymbol{L_G}+\boldsymbol{G}\right)\boldsymbol{z} + c_v\left[\frac{1}{2a}\left\|\boldsymbol{\delta}\right\|^2 + \frac{a}{2}\left\|\boldsymbol{P}\left(\boldsymbol{L_G}+\boldsymbol{G}\right)\boldsymbol{z}\right\|^2\right], \tag{13}$$

where $\|\cdot\|$ is the Euclidean norm. A coefficient $\eta > 0$ is introduced to bound the state measurement error expressed as

$$\left\|\boldsymbol{\delta}\right\| \le \eta\left\|\boldsymbol{P}\left(\boldsymbol{L_G}+\boldsymbol{G}\right)\boldsymbol{z}\right\| = \eta\left\|\boldsymbol{P}\hat{\boldsymbol{e}}_{\boldsymbol{v}}\right\|. \tag{14}$$

Considering that the communication digraph for distributed secondary voltage control has a spanning tree and at least one root DG is given the voltage reference, the symmetric matrix $\boldsymbol{H}$ = $\boldsymbol{P}(\boldsymbol{L_G}+\boldsymbol{G})+(\boldsymbol{L_G}+\boldsymbol{G})^T\boldsymbol{P}$ is a positive definite [18]. Then, we have

$$\left\|\boldsymbol{P}\left(\boldsymbol{L_G}+\boldsymbol{G}\right)\boldsymbol{z}\right\|^2 \le \boldsymbol{z}^T\boldsymbol{H}\boldsymbol{H}\boldsymbol{z} \le \lambda_n\boldsymbol{z}^T\boldsymbol{H}\boldsymbol{z}, \tag{15}$$

where λ_n is the largest eigenvalue of $\boldsymbol{H}$. Hence, the combination of (13)-(15) yields

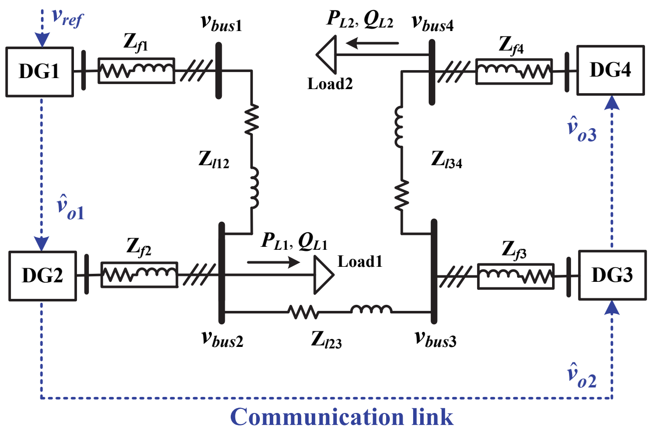

Fig. 4. Microgrid with four DG units.

TABLE I
SYSTERM PARAMETERS

	Parameters	Values
Electrical	Rated Microgrid Frequency	$f = 50$ Hz
	Rated Microgrid Voltage (line-line)	$v_{ref} = 380$ V
	Feeder/Line Impedance	$Z_{f1} = Z_{f3} = 0.02\ \Omega$,0.05mH $Z_{f2} = Z_{f4} = 0.035\ \Omega$,0.08mH $Z_{l12} = Z_{l34} = 0.2\ \Omega$,1mH $Z_{l23} = 0.35\ \Omega$,1.5mH
	Load (per phase)	$P_{L1} = 12$ kW, $Q_{L1} = 8$ kvar $P_{L2} = 15$ kW, $Q_{L2} = 15$ kvar
Control	LPF Bandwidth	$\omega_c = 2\pi\times10$ rad/s
	Frequency Droop Coefficient	$m_{p1} = m_{p2} = 1\times10^{-4}$ rad/(s·W) $m_{p3} = m_{p4} = 0.8\times10^{-4}$ rad/(s·W)
	Voltage Droop Coefficient	$n_{q1} = n_{q2} = 1.3\times10^{-3}$ V/var $n_{q3} = n_{q4} = 1\times10^{-3}$ V/var
	Secondary Voltage Control Gain	$c_v = 5\text{s}^{-1}$
	Tolerance	$\varepsilon = 0.1$

$$\begin{aligned}\dot{V} &\leq -c_v \boldsymbol{z}^T \boldsymbol{P}\left(\boldsymbol{L_G}+\boldsymbol{G}\right)\boldsymbol{z} + c_v\lambda_n\left(\frac{\eta^2}{2a}+\frac{a}{2}\right)\boldsymbol{z}^T\boldsymbol{Hz} \\ &= -\frac{c_v}{2}\left[1-\lambda_n\left(\frac{\eta^2}{a}+a\right)\right]\boldsymbol{z}^T\boldsymbol{Hz}\end{aligned} \quad . \tag{16}$$

(16) is negative if it satisfies

$$\lambda_n\left(\frac{\eta^2}{a}+a\right)<1\,, \tag{17}$$

or equivalently

$$\eta^2 < -a^2+\frac{a}{\lambda_n} = -\left(a-\frac{1}{2\lambda_n}\right)^2+\frac{1}{4\lambda_n^2}\,. \tag{18}$$

η has an upper bound, as shown in (18). If a large value is selected for η, a large state measurement error $\boldsymbol{\delta}$ is allowed from (14) and few events will be triggered. Thus, the upper bound of η is selected as $1/(2\lambda_n)$ to ensure $\dot{V}<0$. In this case, $a = 1/(2\lambda_n)$.

Based on the above analysis, the DG output voltage amplitude v_{oi} asymptotically goes to reference v_{ref} by enforcing the condition (14). However, each DG unit has to identify global state measurement error $\boldsymbol{\delta}$ to check this condition. To determine the event time instants in a distributed manner, a much strict condition is given as

$$\left|\delta_i\right| \leq \frac{\eta}{w_i}\left|\hat{e}_{vi}\right|, \qquad i=1,2,\ldots,n\,. \tag{19}$$

Then, (14) is satisfied because each entry of state measurement error vector $\boldsymbol{\delta}$ is bounded.

An event for the i-th DG unit is triggered when (19) is violated. The i-th DG unit updates $\hat{v}_{oi}$ by sampling output voltage v_{oi} at the event time instant, which resets state measurement error δ_i to zero. Thus, (19) is satisfied to guarantee $\dot{V}<0$. Hence, based on the definition in (9), the proposed distributed event condition is given as

$$\left|\hat{v}_{oi}\left(t\right)-v_{oi}\left(t\right)\right| \geq \frac{\eta}{w_i}\left|\hat{e}_{vi}\right|+\varepsilon\,, \tag{20}$$

where ε is a tolerance with a small value to prevent unnecessarily triggered events due to measurement errors in practical systems. With (20), the event time instants for each DG units can be obtained based on its own and its neighbor voltage information, which is similar with controller design.

The control block diagram of the proposed event-triggered scheme for distributed secondary voltage control is shown in Fig. 3. The event condition determines the event time instants using the states of v_{oi}, $\hat{v}_{oi}$, and $\hat{e}_{vi}$, and generates a signal to trigger the sampling and transmission of voltage state. DG units also receives state $\hat{v}_{oj}$ from the neighbors to update $\hat{e}_{vi}$. The resultant compensation signal V_i^* is provided to the primary control for voltage restoration.

IV. CASE STUDY

An islanded microgrid system with four DG units is investigated in MATLAB/Simulink to validate the effectiveness of the proposed secondary voltage control with event-triggered scheme. The system configuration of power network and communication structure is shown in Fig. 4. Each DG unit is connected to the bus through an RL feeder, and the buses are connected by RL transmission lines. The system parameters are listed in Table I. The droop control without communication is implemented for real and reactive power regulation. The communication links transmit the voltage states of DG units to support the distributed secondary voltage control. DG1 is the only DG unit that is given the voltage reference v_{ref}, and $g_1 = 1$ is the only non-zero pinning gain. The Laplacian matrix of communication digraph associated with the topology shown in Fig. 4 is

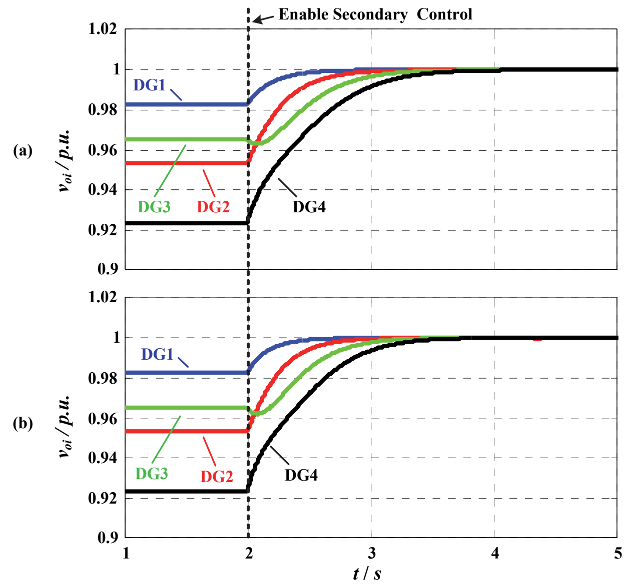

Fig. 5. DG output voltage magnitudes (a) time-triggered scheme; (b) proposed event-triggered scheme.

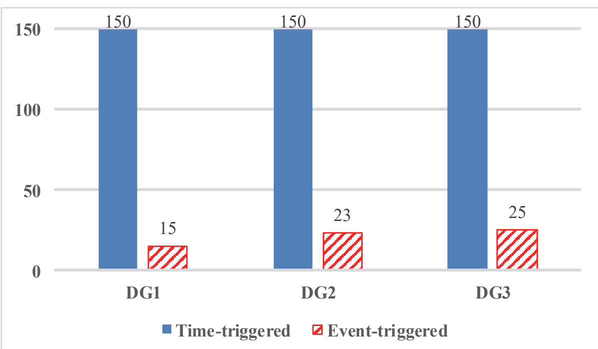

Fig. 6. Number of communication transmissions.

$$L_G = \begin{bmatrix} 0 & 0 & 0 & 0 \\ -1 & 1 & 0 & 0 \\ 0 & -1 & 1 & 0 \\ 0 & 0 & -1 & 1 \end{bmatrix}. \tag{21}$$

The performance of distributed secondary voltage control is demonstrated in Fig. 5. With conventional periodic time-triggered scheme, DG unit sends its measured output voltage every 20 ms. Initially, the microgrid operates in islanded mode, and the voltages deviate from nominal value due to the droop characteristic of the primary control. The secondary voltage control is activated at $t = 2$ s, which gradually shifted up the DG output voltages. The same procedure is conducted with the proposed event-triggered scheme. The waveforms showed that the steady-state and transient responses are practically unaffected. The proposed event-triggered scheme is also effective to restore the output voltages to 1 p.u. and eliminate the voltage deviation. The two schemes synchronized all DG output voltages to reference v_{ref} in about 2 s.

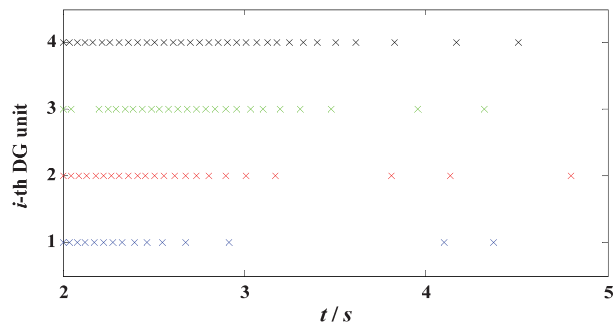

Fig. 7. Event time instants of each DG unit.

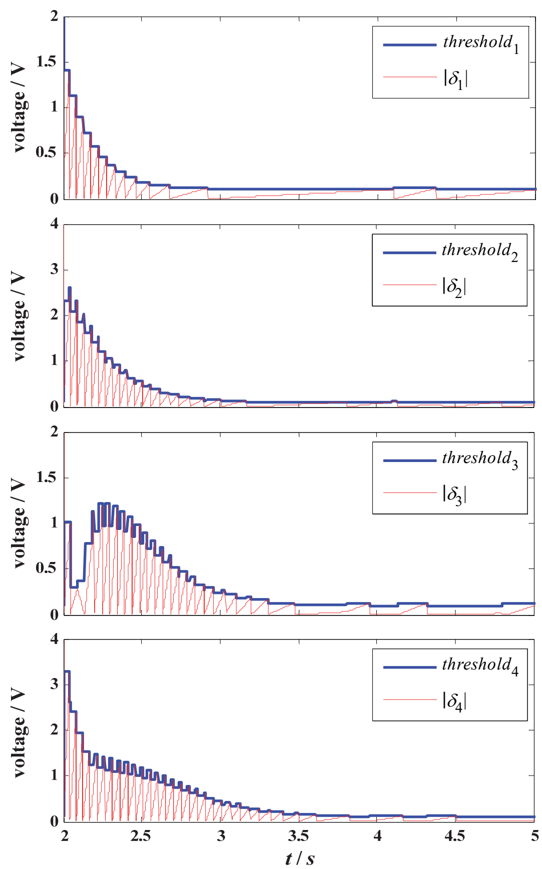

Fig. 8. Evolutions of absolute voltage measurement errors.

The number of communication transmissions for DG units from $t = 2$ s to $t = 5$ s under two secondary voltage control schemes are compared in Fig. 6. In time-triggered scheme, the voltage information is transmitted at a frequency of 50 Hz, which resulted in 150 numbers of transmission for each DG unit in 3 s. With the proposed event-triggered scheme, the DG unit transmitted the voltage information only when its event occurred, which required few number of transmissions. According to (20), the number of communication transmissions in the proposed scheme is mainly affected by the communication topology, initial voltage value of DG units, and tolerance ε. The results in Figs. 5 and 6 indicated that the proposed secondary voltage control has the advantage

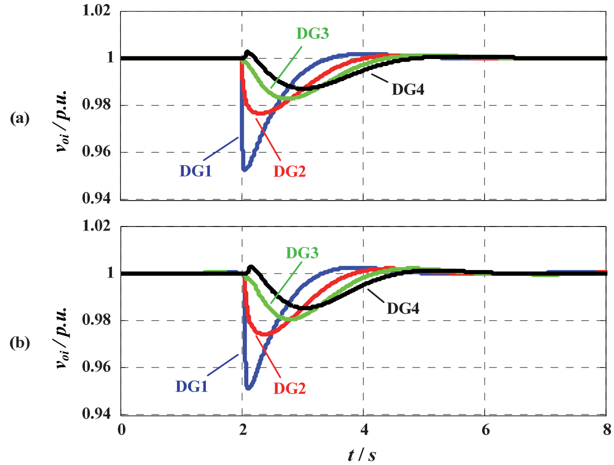

Fig. 9. DG output voltage magnitudes during load change (a) time-triggered scheme; (b) proposed event-triggered scheme.

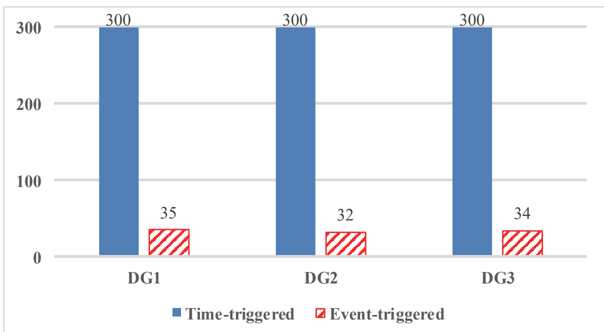

Fig. 10. Numbers of communication transmission during load change.

of reducing communication load without degrading system performance.

The event time instants of each DG unit with the proposed scheme are shown in Fig. 7. Initially, the events occurred frequently due to large differences between DG output voltages and reference value. Thus, good dynamic performance can be achieved. Few events are generated with DG voltages gradually converging to v_{ref} and the system finally operating in steady-state, which indicated an efficient use of communication resources.

Fig. 8 depicts the evolution for the absolute value of voltage measurement error for each DG unit with the proposed scheme. The threshold denotes the right-hand part of (20), which bounds the absolute voltage measurement error $|\delta_i|$. When the threshold is reached, $|\delta_i|$ is reset to zero because an event is triggered and a new sampling of output voltage is executed. The threshold for each DG unit depended on its own voltage state and also on its neighbor voltage information. The thresholds asymptotically approached tolerance ε in steady-state.

To evaluate the proposed scheme, a load changing scenario is conducted. Initially, the islanded microgrid operated in steady-state. At t = 2 s, a 10 kW/8 kvar (per phase) load is added to Bus1. The waveforms of DG output voltage magnitudes and the number of communication transmissions from t = 2 s to t = 8 s are shown in Figs. 9 and 10, respectively. The proposed scheme restored the voltages to the reference with only about one-tenth of the communication numbers for the conventional time-triggered scheme and maintained a good performance.

V. Conclusion

An event-triggered scheme for distributed secondary voltage control with multi-agent consensus algorithm is proposed. Compared with the existing time-triggered controller, the proposed scheme had the advantage of reducing the amount of communication among DG units without degrading the performance of voltage restoration. A fully distributed event condition is developed using Lyapunov technique to facilitate that each DG unit only requires its own and neighbor information to determine the event time instants. The communication transmission is executed aperiodically when an event occurred, and the unnecessary utilization of limited network bandwidth is avoided. Simulation results are presented to verify the effectiveness of the proposed control scheme.

Acknowledgment

This work is supported by National Natural Science Foundation of China (51407173), Zhejiang Provincial Natural Science Foundation for Youths (LQ17E070003), and Young Staff Startup Research Foundation of China Jiliang University (01101/000520).

References

[1] X. Wang, J. M. Guerrero, F. Blaabjerg, and Z. Chen, "A review of power electronics based microgrids," *Journal of Power Electronics*, Vol. 12, No. 1, pp. 181-192, Jan. 2012.

[2] D. E. Olivares, A. Mehrizi-Sani, A. H. Etemadi, C. A. Cañizares, R. Iravani, M. Kazerani, A. H. Hajimiragha, O. Gomis-Bellmunt, M. Saeedifard, R. Palma-Behnke, G. A. Jimenez-Estevez, N. D. Hatziargyriou, "Trends in microgrid control," *IEEE Trans. Smart Grid*, Vol. 5, No. 4, pp. 1905-1919, Jul. 2014.

[3] M. R. Miveh, M. F. Rahmat, A. A. Ghadimi, and M. W. Mustafa, "Power quality improvement in autonomous microgrids using multi-functional voltage source inverters: A comprehensive review," *Journal of Power Electronics*, Vol. 15, No. 4, pp. 1054-1065, Jul. 2015.

[4] J. M. Guerrero, M. Chandorkar, T. Lee, and P. C. Loh, "Advanced control architectures for intelligent microgrids part I: Decentralized and hierarchical control," *IEEE Trans. Ind Electron.*, Vol. 60, No. 4, pp. 1254-1262, Apr. 2013.

[5] J. M. Guerrero, J. C. Vasquez, J. Matas, L. Vicuna, and M. Castilla, "Hierarchical control of droop-Controlled AC and DC microgrids: A general approach toward standardization," *IEEE Trans. Ind Electron.*, Vol. 58, No. 1, pp. 158-172, Jan. 2011.

[6] A. Bidram and A. Davoudi, "Hierarchical structure of microgrids control system," *IEEE Trans. Smart Grid*, Vol. 3, No. 4, pp. 1963-1976, Dec. 2012.

[7] H. Han, X. Hou, J. Yang, J. Wu, M. Su, and J. M. Guerrero, "Review of power sharing control strategies for islanding operation of AC microgrids," *IEEE Trans. Smart Grid*, Vol. 7, No. 1, pp. 200-215, Jan. 2016.

[8] G. Ding, F. Gao, R. Li, and B. Wu, "A communicationless PCC voltage compensation using an improved droop control scheme in Islanding microgrids," *Journal of Power Electronics*, Vol. 17, No. 1, pp. 294-304, Jan. 2017.

[9] Q. Yang, J. A. Barria, and T. C. Green, "Communication infrastructures for distributed control of power distribution networks," *IEEE Trans. Ind. Informat.*, Vol. 7, No. 2, pp. 316-327, May 2011.

[10] R. A. Gupta and M. Y. Chow, "Networked control system: Overview and research trends," *IEEE Trans. Ind Electron.*, Vol. 57, No. 7, pp. 2527-2535, Jul. 2010.

[11] M. Yazdanian and A. Mehrizi-Sani, "Distributed control techniques in microgrids," *IEEE Trans. Smart Grid*, Vol. 5, No. 6, pp. 2901-2909, Nov. 2014.

[12] Q. Shafiee, J. M. Guerrero, and J. C. Vasquez, "Distributed secondary control for islanded microgrids - a novel approach," *IEEE Trans. Power Electron.*, Vol. 29, No. 2, pp. 1018-1031, Feb. 2014.

[13] C. Ahumada, R. C. X. E, Rdenas, D. S. X. E, Ez, and J. M. Guerrero, "Secondary control strategies for frequency restoration in islanded microgrids with consideration of communication delays," *IEEE Trans. Smart Grid*, Vol. 7, No. 3, pp. 1430-1441, May 2016.

[14] F. Guo, C. Wen, J. Mao, and Y. Song, "Distributed secondary voltage and frequency restoration control of droop-controlled inverter-based microgrids," *IEEE Trans. Ind Electron.*, Vol. 62, No. 7, pp. 4355-4364, Jul. 2015.

[15] V. Nasirian, Q. Shafiee, J. M. Guerrero, F. L. Lewis, and A. Davoudi, "Droop-Free distributed control for AC microgrids," *IEEE Trans. Power Electron.*, Vol. 31, No. 2, pp. 1600-1617, Feb. 2016.

[16] J. W. Simpson-Porco, Q. Shafiee, F. Dörfler, J. C. Vasquez, J. M. Guerrero, and F. Bullo, "Secondary frequency and voltage control of islanded microgrids via distributed averaging," *IEEE Trans. Ind Electron.*, Vol. 62, No. 11, pp. 7025-7038, Nov. 2015.

[17] A. Bidram, A. Davoudi, F. L. Lewis, and J. M. Guerrero, "Distributed cooperative secondary control of microgrids using feedback linearization," *IEEE Trans. Power Syst.*, Vol. 28, No. 3, pp. 3462-3470, Aug. 2013.

[18] A. Bidram, A. Davoudi, F. L. Lewis, and Z. Qu, "Secondary control of microgrids based on distributed cooperative control of multi-agent systems," *IET Gener. Transm. Distrib.*, Vol. 7, No. 8, pp. 822-831, Aug. 2013.

[19] D. V. Dimarogonas, E. Frazzoli, and K. H. Johansson, "Distributed event-triggered control for multi-agent systems," *IEEE Trans. Autom. Control*, Vol. 57, No. 5, pp. 1291-1297, May 2012.

[20] H. Zhang, G. Feng, H. Yan, and Q. Chen, "Observer-based output feedback Event-Triggered control for consensus of multi-agent systems," *IEEE Trans. Ind Electron.*, Vol. 61, No. 9, pp. 4885-4894, Sept. 2014.

[21] M. Tahir and S. K. Mazumder, "Self-triggered communication enabled control of distributed generation in microgrids," *IEEE Trans. Ind. Informat.*, Vol. 11, No. 2, pp. 441-449, Apr. 2015.

[22] Y. Fan, G. Hu, and M. Egerstedt, "Distributed reactive power sharing control for microgrids with event-triggered communication," *IEEE Trans. Control Syst. Technol.*, Vol. 25, No. 1, pp. 118-128, Jan. 2017.

[23] C. Dou, D. Yue, and J. M. Guerrero, "Multiagent system-based event-triggered hybrid controls for high-security hybrid energy generation systems," *IEEE Trans. Ind. Informat.*, Vol. 13, No. 2, pp. 584-594, Apr. 2017.

[24] C. Li, X. Yu, W. Yu, T. Huang, and Z. W. Liu, "Distributed event-triggered scheme for economic dispatch in smart grids," *IEEE Trans. Ind. Informat.*, Vol. 12, No. 5, pp. 1775-1785, Oct. 2016.

[25] R. Olfati-Saber and R. M. Murray, "Consensus problems in networks of agents with switching topology and time-delays," *IEEE Trans. Autom. Control*, Vol. 49, No. 9, pp. 1520-1533, Sept. 2004.

[26] W. Ren and R. W. Beard, "Consensus seeking in multiagent systems under dynamically changing interaction topologies," *IEEE Trans. Autom. Control*, Vol. 50, No. 5, pp. 655-661, May 2005.

[27] J. M. Guerrero, L. Garcia De Vicuna, J. Matas, M. Castilla, and J. Miret, "A wireless controller to enhance dynamic performance of parallel inverters in distributed generation systems," *IEEE Trans. Power Electron.*, Vol. 19, No. 5, pp. 1205-1213, Sept. 2004.

Qian Guo was born in Henan, China. She received her B.S. and Ph.D. degrees in Electrical Engineering from Zhejiang University, Hangzhou, China in 2010 and 2016, respectively. She is currently a lecturer in the College of Mechanical and Electrical Engineering, China Jiliang University, Hangzhou, China. Her research interests include control of inverters in microgrids and distributed generation systems.

Hui Cai was born in Zhejiang, China in 1980. He received his B.S.E.E. and Ph.D. degrees from Zhejiang University, Hangzhou, China, in 2002 and 2008, respectively. He is currently working as an associate professor in the College of Mechanical and Electrical Engineering, China Jiliang University, Hangzhou, China. His research interests include power converter systems, ac drives, and new energy power generation.

Ying Wang was born in Henan, China. She received her M.S. degree in Electrical Engineering from North China Electrical University, Baoding, China, in 2004. She is currently a lecturer in the College of Mechanical and Electrical Engineering, China Jiliang University, Hangzhou, China. Her research interests include protection and control in microgrids and distributed generation systems.

Weimin Chen was born in Jiangxi, China. He received his M.S. and Ph.D. degrees in Electrical Engineering from Shanghai University, Shanghai, China, in 2006 and 2011, respectively. He is currently an associate professor in the College of Mechanical and Electrical Engineering, China Jiliang University, Hangzhou, China. His research interests include control of inverters and PV generation.